



## OPEN

## Redox-active charge carriers of conducting polymers as a tuner of conductivity and its potential window

SUBJECT AREAS:  
SENSORS  
POLYMER CHARACTERIZATION  
CHEMICAL PHYSICS  
POLYMERS

Han-Saem Park, Seo-Jin Ko, Jeong-Seok Park, Jin Young Kim &amp; Hyun-Kon Song

i-School of Green Energy, UNIST, Ulsan 689-798, Korea.

Received  
20 June 2013Accepted  
30 July 2013Published  
16 August 2013Correspondence and  
requests for materials  
should be addressed to  
J.Y.K. (jykim@unist.ac.  
kr) or H.-K.S.  
(philiphobi@hotmail.  
com)

Electric conductivity of conducting polymers has been steadily enhanced towards a level worthy of being called its alias, “synthetic metal”. PEDOT:PSS (poly(3,4-ethylenedioxythiophene) doped with poly(styrene sulfonate)), as a representative conducting polymer, recently reached around  $3,000 \text{ S cm}^{-1}$ , the value to open the possibility to replace transparent conductive oxides. The leading strategy to drive the conductivity increase is solvent annealing in which aqueous solution of PEDOT:PSS is treated with an assistant solvent such as DMSO (dimethyl sulfoxide). In addition to the conductivity enhancement, we found that the potential range in which PEDOT:PSS is conductive is tuned wider into a negative potential direction by the DMSO-annealing. Also, the increase in a redox-active fraction of charge carriers is proposed to be responsible for the enhancement of conductivity in the solvent annealing process.

PEDOT:PSS is one of the most well-known conducting polymers due to its high conductivity, high optical transparency, high thermal stability, high mechanical flexibility and high water solubility. The characteristic properties enabled the conducting polymer as transparent electrodes or current collectors of various optoelectronic devices such as solar cells, light-emitting diodes, liquid crystal displays and touch panel displays<sup>1,2</sup>. The conductivity of PEDOT:PSS have increased steadily, recently reaching  $3,065 \text{ S cm}^{-1}$ <sup>3</sup> which is the value to enable PEDOT:PSS to replace widely used transparent conductive oxides such as indium tin oxide or fluorine-doped tin oxide. The primary method to increase conductivity is the *solvent annealing* in which a solvent molecule such as DMSO is introduced into an aqueous solution of PEDOT:PSS and then the mixture is processed into the form of interest like films. Various organic compounds were used as the assistant solvent such as DMSO, alcohols, ionic liquids and anionic surfactant<sup>4–9</sup>. The driving force to enhance conductivity has been proposed as (1) charge screening of the interaction between PEDOT and its dopant (PSS) by the organic compounds<sup>4</sup>, (2) enhanced interchain interaction between PEDOT chains due to their conformational transformation from benzoid-favoring coil structure to quinoid-favoring linear or extended coil structure caused by incorporation of organic molecules interacted with PEDOT as well as PSS<sup>5,10</sup> and (3) development of 3D conducting network associated with exclusion or reduction of excess PSS from conductive PEDOT:PSS domains<sup>6,11,12</sup>. With additional post-treatment of solvent-annealed PEDOT:PSS, highly conductive film ( $1,418 \text{ S cm}^{-1}$ ) was obtained<sup>13</sup>. The film made from ethylene glycol-containing PEDOT:PSS aqueous solution was thermally annealed and then immediately immersed in a solution of the same organic compound. The highest value ( $3,065 \text{ S cm}^{-1}$ ) was obtained by post-treating as-prepared PEDOT:PSS film with  $\text{H}_2\text{SO}_4$  at  $160^\circ\text{C}$ <sup>3</sup>. The anionic  $\text{HSO}_4^-$  functioned as the *secondary dopant* for PEDOT like tosylate<sup>9</sup>, showing the effects similar to those of organic compounds used in solvent annealing.

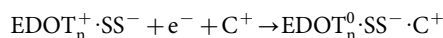
The research focus of the solvent annealing of PEDOT:PSS has been made on how to improve electric conductivity and how the organic molecules or additives work. Rather than the *electric* properties, in this work, we investigated on the change of *electrochemical* properties induced by solvent annealing. That is to say, we moved focus from the level of electric conductivity (ordinate view) to the range of potential in which the electric conductivity maintains (abscissa view).

## Results

**Widening conductive potential window.** Conducting polymers including polypyrroles, polyanilines and polythiophenes (e.g., PEDOT) are prepared by oxidizing corresponding monomers. They have positive charges every three to five monomeric units along polymeric backbone. The positively charged ensembles work as a charge carrier for conduction. During synthesis, counter-anions called dopants are introduced into



the conducting polymers to neutralize the positive charges of backbones. PSS functions as a polyanionic dopant in PEDOT:PSS. The conducting polymers intrinsically in a doped or oxidized state turn electrically insulating when being reduced by applying negative potentials. During reduction, the cationic charge carriers of conducting polymers are lost. Simultaneously, small-sized dopant molecules are effluxed from the films while foreign cations are influxed from electrolyte to the films in presence of large-sized dopants such as PSS:



(doped or oxidized state)                      (dedoped or reduced state)                      (1)

**Conductive**

**Insulating**

where EDOT = the monomeric unit of PEDOT,  $n$  = number of EDOT,  $\text{SS}^-$  = styrenesulfonate of PSS,  $e^-$  = electron and  $\text{C}^+$  = cation in electrolyte.

Therefore, shifting the reduction potential ( $E^0$ , estimated by  $E_{1/2} = (E_{\text{pa}} + E_{\text{pc}})/2$  with  $E_{\text{pa}}$  and  $E_{\text{pc}}$  as anodic and cathodic peak potentials in cyclic voltammograms, respectively) of PEDOT to a more negative value extends the conductive potential window by keeping PEDOT in its oxidized state. The wider conductive range is beneficial when the conductive polymer is used as electrodes of electric double layer capacitors (EDLCs)<sup>14</sup>, electrolytic capacitors<sup>15</sup>, sensors<sup>16</sup> and other electrochemical applications<sup>17</sup>. Various factors determine the value of  $E^0$ . Higher degree of polymerization or molecular weight leads to more negative  $E^0$ : e.g., the values of  $E^0$  decreased from 2.0 V (all potentials are reported versus Ag/AgCl) for thiophene as a monomer

to 1.3 V for its dimer to 1.0 V for its trimer to 0.7 V for its polymer<sup>18</sup>. Structural modification of monomeric unit would be the first choice to control the  $E^0$ . The reduction potential of conducting polymers was controlled by substituents attached to the 3 and 4 positions of thiophene: from more positive than +0.5 V with polythiophene to +0.3 V with poly(3,4-dimethoxythiophene) or -0.2 V with PEDOT:tosylate in 0.1 M tetrabutylammonium perchlorate in acetonitrile<sup>19</sup>. The negative shift of  $E^0$  is caused by electron-donating properties of the alkoxy moieties. The choice of solvent also affects the values of  $E^0$ . +1.24 V and +0.84 V were measured as anodic peak potential of poly(3-methyl thiophene) with 0.1 M  $\text{LiClO}_4$  in glycol and acetonitrile, respectively.

Even without any modification of monomeric units as well as any control of molecular weight in an identical electrolyte, cyclic voltammograms of bare and solvent-annealed PEDOT:PSS (-DMSO and +DMSO) showed that the extension of conductive window of PEDOT:PSS can be achieved by solvent annealing as a simple and versatile strategy to control  $E^0$  (Fig. 1). Three different PEDOT:PSS films were tested, which are prepared from commercially available aqueous solution of PEDOT:PSS: AI4083, PH and PH1000. 5% (or 50%) of DMSO were added to the aqueous solution, followed by drop casting on carbon electrodes. Almost identical electrochemical properties were obtained with both 5% and 50% DMSO. Without solvent annealing (-DMSO), the electric conductivity was estimated by four point probe measurement at  $6.3 \times 10^{-4}$  (0.05)  $\text{S cm}^{-1}$  for AI4083,  $3.8 \times 10^{-3}$  (1.1)  $\text{S cm}^{-1}$  for PH and 0.24 (0.25)  $\text{S cm}^{-1}$  for PH1000 (the values before and in parentheses are the conductivities of the films dried at room temperature and 140°C, respectively). After solvent annealing (+DMSO), the conductivities were markedly enhanced to

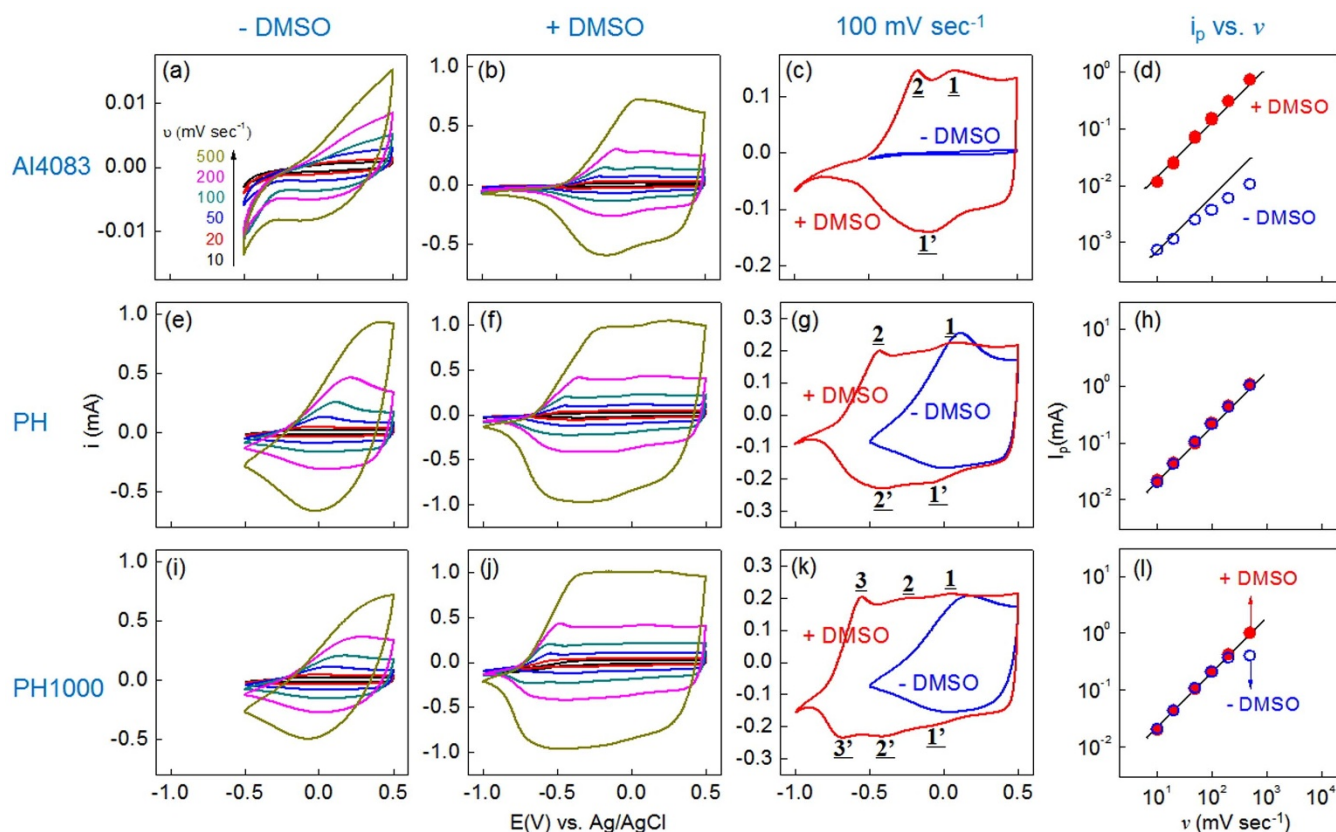


**Figure 1 | Conductive potential window widening of PEDOT:PSS induced by DMSO-annealing.** Cyclic voltammograms (a) to (c), (e) to (g), (i) to (k) and scan-rate ( $v$ ) dependency of peak currents ( $i_p$ ) (d), (h), (l) of three different PEDOT:PSS. The first, second and third rows correspond to AI4083, PH and PH1000, respectively. The first and second columns are for bare (-DMSO) and solvent-annealed (+DMSO) PEDOT:PSS, respectively. The cyclic voltammograms at 100  $\text{mV sec}^{-1}$  are compared between -DMSO and +DMSO of the same PEDOT:PSS in the third column. The values of anodic peak current were used for d to l because cathodic peak current showed similar behaviors in terms of  $v$ -dependency. The lines in figures of the fourth column show the linear relationship with a unity slope indicating that faradaic processes responsible for currents are surface-confined with facile kinetics.

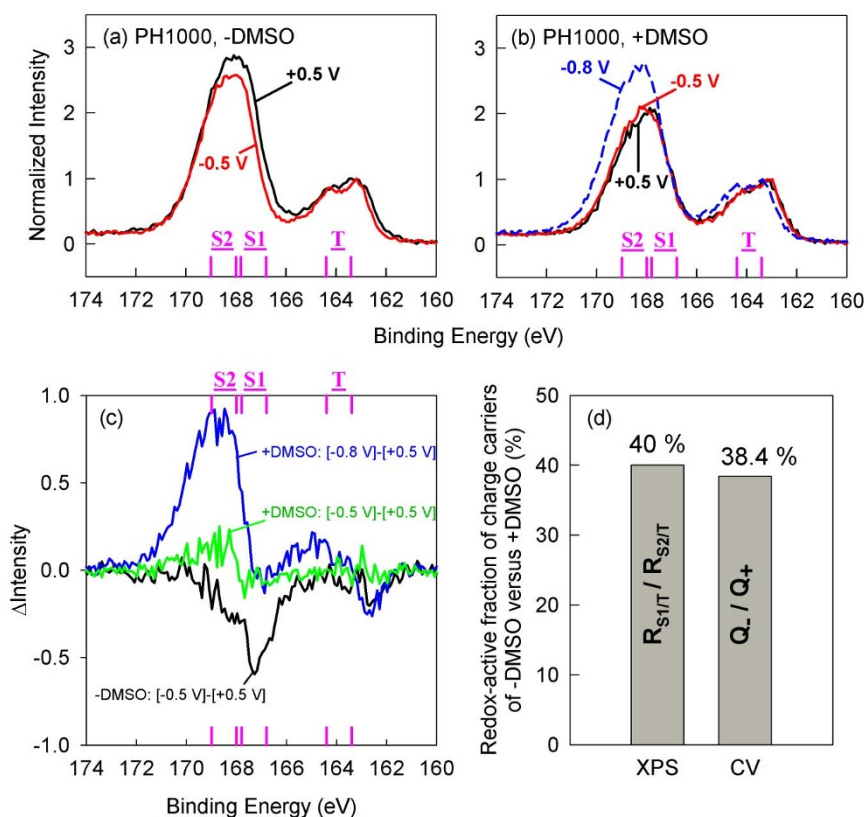


**Figure 2 | Increase of the amount of redox-active charge carriers of PEDOT:PSS induced by DMSO-annealing.** (a) and (b), X-ray photoelectron spectra (XPS) of PH1000 (–DMSO and +DMSO) potentiostatically conditioned at +0.5 V, –0.5 V and –0.8 V. Intensity was normalized by the maximum value of **T** peak. The peak locations of doublets for **T**, **S1** and **S2** were indicated on the abscissa. (c), Spectral change of potentiostatically controlled samples from their fully oxidized states at +0.5 V. Squared brackets indicate the spectrum of PH1000 potentiostatically controlled at the potential indicated within it. (d), –DMSO/+DMSO ratio of the redox-active fraction of total charge carriers estimated spectroscopically from XPS and electrochemically from cyclic voltammograms (CV) in Fig. 1.

15 (870) S cm<sup>−1</sup> for PH and 250 (1,300) S cm<sup>−1</sup> for PH1000 (The conductivity of AI4083 after solvent annealing was difficult to measure because a film was poorly and heterogeneously formed). PH1000, as a representative example, experienced the  $E^0$  shift from +0.15 V to −0.62 V at 100 mV sec<sup>−1</sup>, being conductive in an additional potential range of ~ 0.8 V (Fig. 1k).

The scan-rate dependency of peak currents responsible for oxidation of PEDOT:PSS (Fig. 1d, h, l) showed that solvent-annealed films (+DMSO) follow faithfully the behavior of surface-confined electrochemical processes indicated by a unity slope (slope = 1) in log-log plots (that is to say,  $i_p \propto \nu^1$  with  $i_p$  = peak current and  $\nu$  = scan rate). However, the bare films (–DMSO) exhibited a deviation from the ideal behavior especially at high scan rates. Due to their low electric conductivity, AI4083 and PH1000 films delivered peak currents lower than the values expected from the surface-confined oxidation from 100 mV sec<sup>−1</sup> and 500 mV sec<sup>−1</sup>, respectively. PH film, the conductivity of which is in the level of 10<sup>0</sup> S cm<sup>−1</sup>, ideally behaved in terms of scan-rate dependency.

**Redox-active charge carriers.** With a closer look, the voltammetric curve of solvent-annealed PH1000 (+DMSO) consists of three different redox stages (Fig. 1k):  $E_{pa}/E_{pc}$  = +25 mV/−80 mV for **1**, −230 mV/−420 mV for **2** and −550 mV/−680 mV for **3**. The redox stage **1** is found at the potential roughly identical (or slightly more negative) to the redox of –DMSO (at +150 mV/+30 mV) with the similar current values. Some of peaks are merged in AI4083 and PH prepared in presence of DMSO. As a first guess, therefore, we could hypothesis that DMSO-annealing would generate additional doping sites of different redox potential with

increasing the number of charge carriers. However, the solvent annealing was known not to increase number of charge carriers or doping level but to enhance mobility or hopping rate of the fixed number of carriers existing along polymer backbones (due to conformational change or enhanced 3D conducting network)<sup>10</sup>. Also, carrier densities of all PEDOT:PSS films were estimated around  $2.2 \times 10^{20}$  cm<sup>−3</sup> independent of solvent annealing (Fig. S1 and Table. S1 in Supporting Information). As an alternative hypothesis, the DMSO-annealing leads to additional energetics or redox stages of the identical number of oxidized states. The second interpretation could be supported by the fact that similar values of currents are obtained at the different potentials and also the peaks are merged together without any increase of current in some cases. However, it is still difficult to imagine multiple oxidation states of a fixed redox-active site are possible.

To investigate why those multi-stage redox behavior is found after solvent-annealing, the binding energy of sulfur 2p orbitals (S2p) were traced along reducing passage. Even if many literatures focus simply on the relative ratio of PEDOT to PSS, the S2p peaks can be deconvoluted to three different doublet peaks for EDOT (**T** at 163.4 eV and 164.4 eV), EDOT<sup>+</sup>SS<sup>−</sup> (**S1** at 166.8 eV and 167.8 eV) and H<sup>+</sup>SS<sup>−</sup> (**S2** at 168 eV and 169 eV)<sup>20</sup>. Via reducing the fully oxidized PEDOT:PSS (PH1000 as a representative), significantly different spectral changes of X-ray photoelectron spectra (XPS) were observed between –DMSO and +DMSO (Fig. 2). +DMSO was fully reduced at a more negative potential (−0.8 V) while the reduced state of –DMSO was prepared at −0.5 V as mentioned above (Fig. 1). The decrease of **S1** peak responsible for doping contents was experienced by –DMSO during the reduction. On the



other hand, the increase of **S2** peak was found after full reduction of +DMSO at  $-0.8$  V. At a middle potential ( $-0.5$  V) for +DMSO, there was no significant spectral difference from the fully oxidized sample at  $+0.5$  V, differently from the case of  $-$ DMSO. During reduction, positive charge carrier sites of the polymer backbone are lost so that the electrostatic interaction between  $\text{EDOT}^+$  and  $\text{SS}^-$  becomes weak with the formation of  $\text{H}^+ \cdot \text{SS}^-$ . As shown clearly in the intensity subtraction plot (Fig. 2c), therefore, the decrease in **S1** peak for  $-$ DMSO ( $\Delta\text{S1}$ , negative peaks, black) as well as the increase in **S2** for +DMSO ( $\Delta\text{S2}$ , positive peaks, blue) can be interpreted as dedoping. The dedoping fraction or redox-active portion of dopants during reduction can be quantified by the ratio of peak areas of  $\Delta\text{S1}$  or  $\Delta\text{S2}$  to  $\text{T}$  ( $R_{\text{S1/T}}$  or  $R_{\text{S2/T}}$ ):  $R_{\text{S1/T}} = 1.1373/2.8279 = 40\%$  or  $R_{\text{S2/T}} = 2.6705/2.6783 = 100\%$ . Charge carriers of +DMSO were completely ( $\sim 100\%$ ) reduced while only 40% of the charge carriers were electroactive in  $-$ DMSO. The ratio of  $R_{\text{S1/T}}$  of  $-$ DMSO to  $R_{\text{S2/T}}$  of +DMSO consists with the ratio of charges stored in  $-$ DMSO to +DMSO ( $Q_-/Q_+$ ) as shown in cyclic voltammograms (Fig. 1k):  $Q_-/Q_+ = 22.4 \text{ C g}^{-1}/58.2 \text{ C g}^{-1} = 38.4\%$  for the cathodic process (Fig. 2d). That is to say, the amount of redox-active charge carriers of +DMSO would be 2.5 times larger than that of  $-$ DMSO, even if there were no difference of doping level between  $-$ DMSO and +DMSO in a fully oxidized state. Therefore, we could conclude that all redox stages including **1**, **2** and **3** work electrochemically in the conformation induced by solvent-annealing (linear or extended coil configuration) while only redox stage **1** is electrochemically active in the bare PEDOT:PSS. DMSO or equivalent assistant solvent molecules function as a potion to revive dead charge carriers in terms of electrochemical activity. Charge screening of the interaction between PEDOT and its dopant (PSS) by the organic compounds<sup>4</sup> could make dedoping process thermodynamically more comfortable. Also, the enhanced connectivity of conductive pathways<sup>6,11,12</sup> would enable electron to reach all of the potentially redox-active sites.

The conductivity enhancement by solvent-annealing also can be interpreted in terms of the redox-active doping level or the number of redox-active charge carriers. From the discussion above, the solvent-annealing increases the number of redox-active charge carriers from 40% utility to  $\sim 100\%$  utility of total number of intrinsic charge carriers. There is every possibility that only the redox-active charge carriers are responsible efficiently for electric conductivity, considering that the positive charge carriers of  $\text{EDOT}_n^+$  accept electrons during conduction like transient reduction. Conductivities ( $\sigma$ ) come from the product of mobility ( $\mu$ ) and carrier density ( $n$ ). Due to a disorder broadening of energy levels of charge carriers,  $\mu$  is the function of  $n$  with an approximate linearity in log-log scale of a specific range of  $n$ <sup>21,22</sup>:

$$\sigma \propto n\mu \propto nn^b = n^{b+1} = n^\beta \quad (2)$$

When the number of redox-active charge carriers is used for  $n$  instead of total number of charge carriers detected by non-electrochemical method (reflectance spectra), the empirical relationship approximated the conductivity enhancement ratio of PEDOT:PSS with  $b = 7 \sim 8$  with poly(3-hexylthiophene) from the literatures<sup>21,22</sup>. For example, the increase of redox-active carrier density estimated at 2.5 times (100% utility of +DMSO versus 40% of  $-$ DMSO for PH1000) leads to the conductivity enhancement of  $(2.5)^8 \sim 9 = \sim 10^3$  order of magnitude. The enhancement factor is consistent with the value obtained by conductivity measurement:  $0.24 \text{ S cm}^{-1}$  for  $-$ DMSO versus  $250 \text{ S cm}^{-1}$  for +DMSO of PH1000.

$-$ DMSO and +DMSO were compared in terms of equivalent circuit parameters by electrochemical impedance spectroscopy (Fig. 3 and Table S2 in Supporting information). At  $+0.5$  V where both of PEDOT:PSS is conductive, both  $-$ DMSO and +DMSO showed the qualitatively same capacitive behaviors normally obtained from conductive porous structures with  $45^\circ$ -inclined line at higher frequencies and near-but-not- $90^\circ$  line at lower frequencies<sup>23-25</sup> +DMSO samples

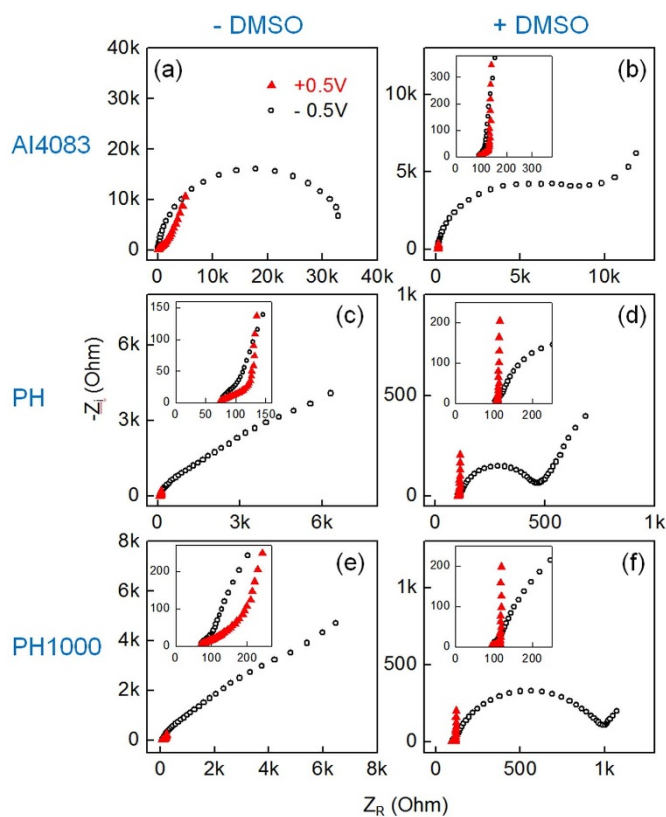


**Figure 3 | Electrochemical impedance spectra of PEDOT:PSS.** (a) and (b), AI4083. (c) and (d), PH. (e) and (f), PH1000. The left and right columns are for PEDOT:PSS prepared in absence and presence of DMSO ( $-$ DMSO and +DMSO), respectively. Impedance was measured at  $+0.5$  V and  $-0.5$  V as biased potentials every sample from 100 kHz to 0.5 Hz.

showed higher values of capacitance as expected from their superior conductivities. At  $-0.5$  V where +DMSO is conductive but  $-$ DMSO is insulating, clearly different impedance behaviors were obtained. Charge transfer processes caused by reduction of oxidized states and vice versa were observed with +DMSO. On the contrary, diffusion limited processes recognized by Warburg-type impedance were found because the PEDOT:PSS layer works as a porous insulating film.

**Detection of electroactive species.** To clarify the difference between  $-$ DMSO and +DMSO as well as to emphasize why the extension of conductive potential window of conducting polymers is useful, we measured the electrochemical signals of three different electroactive species on electrodes of  $-$ DMSO and +DMSO (Fig. 4).  $\text{K}_3\text{Fe}(\text{CN})_6$  ( $\text{FeCN}$ , 1 mM) shows one electron reversible charge transfer electrochemistry based on  $\text{Fe}^{3+/2+}$ :  $[\text{Fe}(\text{CN})_6]^{3-} + e^- \rightarrow [\text{Fe}(\text{CN})_6]^{4-}$ . Its standard reduction potential ( $E^\circ$ ) is  $+0.27$  V at which both  $-$ DMSO and +DMSO are conductive. Even if electrochemical signals of FeCN are expected to be successfully measured with  $-$ DMSO and +DMSO, the peaks responsible for the faradaic reaction were observed clearer on +DMSO than  $-$ DMSO due to higher conductivity of +DMSO (Fig. 4a). Indigo carmine (IC, 0.25 mM) is electroactive with a proton-involved electrochemical reaction:  $\text{IC} + 2\text{H}^+ + 2e^- \rightarrow \text{ICH}_2$ . Therefore, we controlled pH to adjust its reduction potential ( $E$ ) to the value at which  $-$ DMSO is insulating while +DMSO is conductive. At pH3.5,  $E_{1/2}$  was estimated at  $-0.086$  V on a glassy carbon disk electrode. As expected, the electrochemical signal of IC is detected only on +DMSO (Fig. 4b). The same signals were not found clearly on the

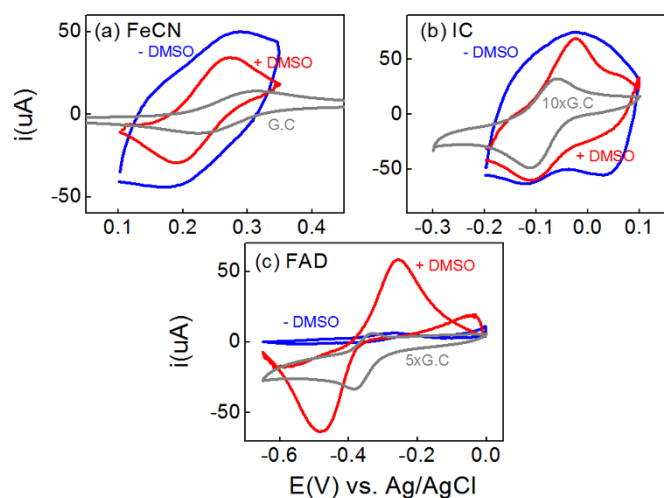


**Figure 4** | Electrochemically detected signals of three different electroactive species (A) on PH1000-filmed electrodes ( $-DMSO$  and  $+DMSO$ ). The net currents were calculated by subtracting the current obtained in A-absent electrolyte ( $-A$ ) from the current obtained in A-present electrolyte ( $+A$ ).  $K_3Fe(CN)_6$  (FeCN, 1 mM, (a)), indigo carmine (IC, 0.25 mM, (b)) and flavin adenine dinucleotide (FAD, 1 mM, (c)) were selected as A. To identify the species responsible for peaks, the cyclic voltammograms obtained on glassy carbon disk electrodes (GC, area =  $3.14 \text{ mm}^2$ ) were also shown with indicated magnifications of current. The raw cyclic voltammograms were provided in Fig. S2 of Supporting Information.

electrodes of  $-DMSO$  because the PEDOT:PSS film is at least partially insulating so that there are less chances of collision between conductive electrode and the electroactive species. As the last electroactive species, a bimolecule was selected, which is used as an electron transfer mediator in enzymes or various biosystems. The electrochemistry of flavin adenine dinucleotide (FAD, 1 mM) also involved proton like IC:  $FAD + H^+ + e^- \rightarrow FADH$  with  $E = -0.36 \text{ V}$  at pH6.0. Not on the insulating electrode ( $-DMSO$ ) but on the conductive electrode ( $+DMSO$ ), FAD was clearly detected (Fig. 4c).

## Discussion

In this work, we reported that the solvent annealing not only increases electric conductivity of PEDOT:PSS but also widens conductive potential window of the conducting polymer. Also, evidences were provided, which support the hypothesis that *electroactive* portion of charge carriers could determine the conductivity of conducting polymers. Even if total number of charge carriers or doping level were unchanged, the solvent annealing would induce the increase of the *electroactive* carriers. The widened conductive potential window of conducting polymers was shown to be utilized as electrodes of chemical sensors.

## Methods

**Materials.** Three different PEDOT:PSS solutions (1.0 ~ 1.7 wt.%) were purchased from Heraeus: AI4083, PH and PH1000. The other reagents were purchased from Sigma-Aldrich.

**Solvent annealing.** 50  $\mu\text{L}$  dimethyl sulfoxide (DMSO) were added to 1 mL of PEDOT:PSS solution, followed by stirring over 2 h.

**Film formation.** The bare or DMSO-containing polymer solutions were casted as a form of film on substrates. They were drop-casted on screen printed carbon electrodes (Sensor R&D, Area =  $19.6 \text{ mm}^2$ ) for electrochemistry or spin-coated on glass substrates for conductivity measurement. The same amount of PEDOT were loaded on the electrodes independent of its kind. The thicknesses of the films were around  $3.5 \text{ }\mu\text{m}$  with less than  $0.5 \text{ }\mu\text{m}$  deviation.

**Conductivity measurement.** Electric conductivities were measured by using a four-point-probe technique (CMT-SR1000N, Advanced Instrument Technology). 1 mL of aqueous solutions of PEDOT:PSS with or without 5 vol.% DMSO were coated on glass substrates ( $1.5 \text{ cm}$  by  $1.5 \text{ cm}$ ) at 1,500 to 2,000 rpm for 60 s and then dried at room temperature for 1 day or  $140^\circ\text{C}$  for 10 min.

**Electrochemical measurement.** Cyclic voltammograms and impedance spectra were measured by using a potentiostat (VMP3, Bio-Logic). Electrochemical measurements were configured with three electrode systems: screen-printed carbon electrodes as working electrodes, Pt flag as a counter electrode and Ag/AgCl (0.197 V vs. NHE) as a reference. 0.1 M  $H_2SO_4$  (aq) was used as electrolyte for measuring redox activity of PEDOT:PSS. Three different electroactive species were used to confirm the conductive windows of  $-DMSO$  and  $+DMSO$ : 1 mM  $K_3Fe(CN)_6$  in 0.2 M NaCl (aq); 0.25 mM indigo carmine in 0.2 M NaCl (aq) at pH 3.5 adjusted by 0.15 mM  $H_2SO_4$ ; and 1 mM flavin adenine dinucleotide in phosphate buffer solution at pH 6.0.

**X-ray photoelectron spectroscopy (XPS).** Prior to XPS measurements (K-alpha, Thermo Fisher), PEDOT:PSS films were conditioned potentiostatically at  $+0.5 \text{ V}$ ,  $-0.5 \text{ V}$  and  $-0.8 \text{ V}$ .

- Na, S.-I., Kim, S.-S., Jo, J. & Kim, D.-Y. Efficient and Flexible ITO-Free Organic Solar Cells Using Highly Conductive Polymer Anodes. *Adv. Mater.* **20**, 4061–4067 (2008).
- Hu, Z., Zhang, J., Hao, Z. & Zhao, Y. Influence of doped PEDOT:PSS on the performance of polymer solar cells. *Sol. Energy Mater. Sol. Cells* **95**, 2763–2767 (2011).
- Xia, Y. J., Sun, K. & Ouyang, J. Y. Solution-Processed Metallic Conducting Polymer Films as Transparent Electrode of Optoelectronic Devices. *Adv. Mater.* **24**, 2436–2440 (2012).
- Kim, J. Y., Jung, J. H., Lee, D. E. & Joo, J. Enhancement of electrical conductivity of poly(3,4-ethylenedioxythiophene)/poly(4-styrenesulfonate) by a change of solvents. *Synth. Met.* **126**, 311–316 (2002).
- Ouyang, J. *et al.* On the mechanism of conductivity enhancement in poly(3,4-ethylenedioxythiophene):poly(styrene sulfonate) film through solvent treatment. *Polymer* **45**, 8443–8450 (2004).
- Crispin, X. *et al.* The origin of the high conductivity of poly(3,4-ethylenedioxythiophene)-poly(styrenesulfonate) (PEDOT-PSS) plastic electrodes. *Chem. Mater.* **18**, 4354–4360 (2006).
- Nardes, A. M., Janssen, R. A. J. & Kemerink, M. A Morphological Model for the Solvent-Enhanced Conductivity of PEDOT:PSS Thin Films. *Adv. Funct. Mater.* **18**, 865–871 (2008).
- Dobbelin, M. *et al.* Influence of ionic liquids on the electrical conductivity and morphology of PEDOT: PSS films. *Chem. Mater.* **19**, 2147–2149 (2007).
- Fan, B. H., Mei, X. G. & Ouyang, J. Y. Significant conductivity enhancement of conductive poly(3,4-ethylenedioxythiophene): Poly(styrenesulfonate) films by adding anionic surfactants into polymer solution. *Macromolecules* **41**, 5971–5973 (2008).
- Ouyang, J. *et al.* High-Conductivity Poly(3,4-ethylenedioxythiophene): Poly(styrene sulfonate) Film and Its Application in Polymer Optoelectronic Devices. *Adv. Funct. Mater.* **15**, 203–208 (2005).
- Jonsson, S. K. M. *et al.* The effects of solvents on the morphology and sheet resistance in poly(3,4-ethylenedioxythiophene)-polystyrenesulfonic acid (PEDOT-PSS) films. *Synth. Met.* **139**, 1–10 (2003).
- Lee, H. J., Lee, J. & Park, S. M. Electrochemistry of Conductive Polymers. 45. Nanoscale Conductivity of PEDOT and PEDOT:PSS Composite Films Studied by Current-Sensing AFM. *J. Phys. Chem. B* **114**, 2660–2666 (2010).
- Kim, Y. H. *et al.* Highly Conductive PEDOT:PSS Electrode with Optimized Solvent and Thermal Post-Treatment for ITO-Free Organic Solar Cells. *Adv. Funct. Mater.* **21**, 1076–1081 (2011).
- Ghosh, S. & Inganäs, O. Conducting Polymer Hydrogels as 3D Electrodes: Applications for Supercapacitors. *Adv. Mater.* **11**, 1214–1218 (1999).
- Kudoh, Y., Akami, K. & Matsuya, Y. Solid electrolytic capacitor with highly stable conducting polymer as a counter electrode. *Synth. Met.* **102**, 973–974 (1999).
- Pan, L. *et al.* Hierarchical nanostructured conducting polymer hydrogel with high electrochemical activity. *Proc. Natl. Acad. Sci. U. S. A.* **109**, 9287–9292 (2012).
- Groenendaal, L. *et al.* Poly(3,4-ethylenedioxythiophene) and Its Derivatives: Past, Present, and Future. *Adv. Mater.* **12**, 481–494 (2000).
- Diaz, A. F. *et al.* Electrooxidation of aromatic oligomers and conducting polymers. *J. Electroanal. Chem.* **121**, 355–361 (1981).
- Zotti, G., Zecchin, S., Schiavon, G. & Groenendaal, L. B. Conductive and Magnetic Properties of 3,4-Dimethoxy- and 3,4-Ethylenedioxy-Capped Polypyrrole and Polythiophene. *Chem. Mater.* **12**, 2996–3005 (2000).
- Crispin, X. *et al.* Conductivity, morphology, interfacial chemistry, and stability of poly(3,4-ethylenedioxythiophene)-poly(styrene sulfonate): A photoelectron spectroscopy study. *J. Polym. Sci., Part B: Polym. Phys.* **41**, 2561–2583 (2003).
- Arkipov, V. I. *et al.* Charge carrier mobility in doped semiconducting polymers. *Appl. Phys. Lett.* **82**, 3245–3247 (2003).
- Jiang, X. *et al.* Doping-induced change of carrier mobilities in poly(3-hexylthiophene) films with different stacking structures. *Chem. Phys. Lett.* **364**, 616–620 (2002).



23. Song, H. K., Hwang, H. Y., Lee, K. H. & Dao, L. H. The effect of pore size distribution on the frequency dispersion of porous electrodes. *Electrochim. Acta* **45**, 2241–2257 (2000).
24. Song, H. K., Jung, Y. H., Lee, K. H. & Dao, L. H. Electrochemical impedance spectroscopy of porous electrodes: the effect of pore size distribution. *Electrochim. Acta* **44**, 3513–3519 (1999).
25. Song, H. K. *et al.* Electrochemical porosimetry. *J. Electrochem. Soc.* **151**, E102–E109 (2004).

## Acknowledgments

This work was supported by MOTIE (Green:10042948(KEIT), Inter-ER:R0000491) and MSIP (CRC: 2013K000210), Korea.

## Author contributions

H.-S.P., J.-S.P.: material preparation and electrochemical characterization and analysis. S.-J.K., J.Y.K.: charge transport characterization. H.-K.S.: data analysis, writing and project planning.

## Additional information

**Supplementary information** accompanies this paper at <http://www.nature.com/scientificreports>

**Competing financial interests:** The authors declare no competing financial interests.

**How to cite this article:** Park, H., Ko, S., Park, J., Kim, J.Y. & Song, H. Redox-active charge carriers of conducting polymers as a tuner of conductivity and its potential window. *Sci. Rep.* **3**, 2454; DOI:10.1038/srep02454 (2013).



This work is licensed under a Creative Commons Attribution-NonCommercial-NoDerivs 3.0 Unported license. To view a copy of this license, visit <http://creativecommons.org/licenses/by-nc-nd/3.0>